Applied Physics A (2020) 126:168
https://doi.org/10.1007/s00339-020-3359-1

Applied Physics A
Materials Science & Processing

The effect of heterovalent doping on the stability and properties of multiferroic Aurivillius phases

Inna V. Lisnevskaya[1] · Vera V. Butova[2,3] · Yury V. Rusalev[2] · Victor V. Shapovalov[2] · Heba Y. Zahran[4,5] · Ibrahim S. Yahia[4,5] · Alexander V. Soldatov[2]

Received: 17 November 2019 / Accepted: 29 January 2020
© Springer-Verlag GmbH Germany, part of Springer Nature 2020

Abstract
The effect of magnetoactive cations on the stability and properties of Aurivillius phases (1) $Bi_5Ti_2(TiFe)_{1-x}(NiNb)_xO_{15}$, (2) $Bi_4Ti_{3-2.5x}(Nb_{1/2}Fe_{1/2})_x(Nb_{2/3}Ni_{1/3})_{1.5x}O_{12}$, (3) $Bi_3Ti_{1-2.5x}Nb_{1+1.5x}(Fe_{1/2}Ni_{1/2})_xO_9$, (4) $Bi_{m+1}Fe_{m-3}Ti_{(3-x)}(Ni_{1/3}Nb_{2/3})_xO_{3m+3}$ has been investigated. The range of existence of solid solutions was found to be limited to the values of $x = 0$–0.10 (1), 0–0.3 (2), and 0–0.2 (3). Although the solid solutions exist in the whole concentration range studied ($x = 0$–0.07) in the series (4), the stability is limited to the value of $m = 6$–7. The unit cell volumes increase with increasing x, which is expected due to the ionic radii of the dopant cations that are larger than those of the substituted cations. The coexistence of piezoelectric and magnetic properties was observed in the samples of solid solutions (1) and (4): the values of the piezoelectric coefficient d_{33} and piezoelectric voltage coefficient g_{33} reach 7 pC/N and 3.5 mV m/N, respectively; the saturation magnetization M_s and remanent magnetization M_r increase with increasing x, while the coercivity remains almost unchanged. Thermal studies indicate phase transitions in $Bi_5Ti_2(TiFe)_{1-x}(NiNb)_xO_{15}$, and $Bi_{m+1}Fe_{m-3}Ti_{(3-x)}(Ni_{1/3}Nb_{2/3})_xO_{3m+3}$ at ~ 300–400, 750 and 840 °C. Additionally, these samples demonstrate a magnetodielectric effect of up to ~ 50% when applying a DC magnetic field of ~ 1 T in the temperature range of ~ 340–350 °C that is supposed to be a ferromagnetic Curie point.

Keywords Multiferroics · Aurivillius phases · Magnetodielectric effect

1 Introduction

Aurivillius phases with the general formula $(A', A'\ldots)_{m+1}(B', B'\ldots)_mO_{3m+3}$ are the family of layered perovskites, which has been known for more than half a century [1–4]. The structure of these compounds is usually described as a sequence of $[A'_2O_2]^{2+}$ layers and perovskite blocks of $[(A', A'\ldots)_{m-1}(B', B'\ldots)_mO_{3m+1}]^{2-}$, where the natural number m corresponds to the number of layers of BO_6 octahedra that form the perovskite blocks. The cubooctahedral A sites with a coordination number of 12 can be occupied by large cations such as Na^+, K^+, Ca^{2+}, Sr^{2+}, Ba^{2+}, Pb^{2+}, Bi^{3+}, Ln^{3+}, while the B sites are suitable for the six-coordinated cations such as Fe^{3+}, Cr^{3+}, Ti^{4+}, Nb^{5+}, W^{6+} that prefer the octahedral geometry. While the perovskite blocks may have considerable variation in composition, the sites in the interblock layers are entirely occupied by Bi^{3+} ions in the form of $[Bi_2O_2]^{2+}$ sheets. Figure 1 shows the unit cells of some well-known layered perovskites.

Aurivillius phases which contain the ferroelectric cations such as Ti^{4+}, Zr^{4+}, Nb^{5+}, Ta^{5+} usually have distorted and polar structures at room temperature and exhibit one or more ferroelectric phase transition at high temperatures. The compounds with magnetic ions (primarily, the iron triad) are involved in phase transitions associated with magnetic ordering. Thus, for example, in the

✉ Inna V. Lisnevskaya
liv@sfedu.ru

1 Faculty of Chemistry, Southern Federal University, Rostov-on-Don, Russia

2 The Smart Materials Research Institute, Southern Federal University, Rostov-on-Don, Russia

3 Federal Research Centre the Southern Scientific Center of the Russian Academy of Sciences, Rostov-on-Don, Russia

4 Advanced Functional Materials & Optoelectronic Laboratory (AFMOL), Department of Physics, Faculty of Science, King Khalid University, P.O. Box 9004, Abha, Saudi Arabia

5 Nanoscience Laboratory for Environmental and Bio-medical Applications (NLEBA), Semiconductor Lab, Physics Department, Faculty of Education, Ain Shams University, Roxy, Cairo 11757, Egypt

Published online: 08 February 2020

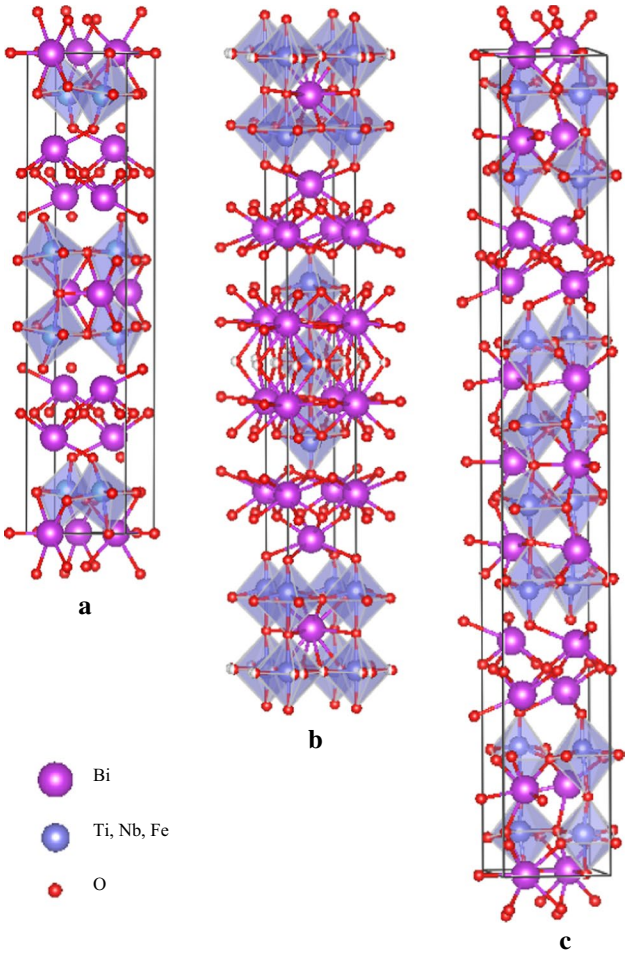

Fig. 1 Crystal structure of Aurivillius phases: **a** Bi_3TiNbO_9, **b** $Bi_4Ti_3O_{12}$, **c** $Bi_5Ti_3FeO_{15}$

$Bi_4Ti_3O_{12}$–$BiFeO_3$ series ($Bi_{m+1}Fe_{m-3}Ti_3O_{3m+3}$), many Aurivillius phases showing both ferroelectric and magnetic properties can be obtained with a various number of layers in perovskite blocks [5]. The combination of ferroelectric and magnetic properties is indirectly associated with the fact that the end members of this solid solution series have magnetic and/or ferroelectric properties: $Bi_4Ti_3O_{12}$ is a ferroelectric with monoclinic symmetry that shows a ferroelectric phase transition at the temperature of 675 °C, while $BiFeO_3$ is an antiferromagnetic and ferroelectric material with rhombohedral symmetry and cycloidal magnetic ordering (ferroelectric and antiferromagnetic point at ~ 850 °C and ~ 370 °C, respectively [6]). In other words, according to the experimental data, the compounds of the $Bi_{m+1}Fe_{m-3}Ti_3O_{3m+3}$ family are multiferroics. For example, it was reported on the magnetoelectric (ME) properties in several-layered perovskites of the $Bi_4Ti_3O_{12}$–$BiFeO_3$ series [7–9]. In particular, four-layered bismuth ferrotitanate $Bi_5FeTi_3O_{15}$ exhibits a record high ME effect for single-phase multiferroics (16 mV/(cm Oe)) at − 190 °C. On average, the ME coefficients for Aurivillius phases are not larger than 10 mV/(cm Oe).

The introduction of magnetically active cobalt and/or nickel cations into the B-sublattice of Aurivillius phases was reported to enhance the magnetic parameters regardless of the composition [10–15]: the remanent magnetization M_r and saturation magnetization M_s are increased twofold or more compared to those of the undoped compounds. Therefore, Co- and/or Ni-containing Aurivillius phases attract much research interest. Thus, Wang et al. [10] have investigated the ceramic samples with the general formula of $Bi_6Fe_{2-x}Co_{x/2}Ni_{x/2}Ti_3O_{18}$ ($0 \le x \le 1$). It was observed that, with $x = 0.4$, these materials exhibit clear ferromagnetism with the maximum remanent magnetization $M_r = 0.5$ emu/g and saturation magnetization $M_s = 2.4872$ emu/g. A similar improvement in magnetic properties was observed by Liu et al. [11] in Ni-containing five-layered perovskite thin films $Bi_6Fe_{2-x}Co_xTi_3O_{18}$ with $x = 0.6$. Shu et al. [12] and Chen et al. [13] have reported on the synthesis of four-layered Aurivillius phases $Bi_4NdTi_3Fe_{1-x}Co_xO_{15}$ ($x = 0.1$, 0.3, 0.5, and 0.7) and $Bi_5Ti_3Fe_{0.5}Ni_{0.5}O_{15}$, respectively. In both cases, the authors observed the ferromagnetic behaviour and the improvement of the magnetic parameters of the materials. In the first case, the best magnetic characteristics were found in the composition with $x = 0.3$. Lei et al. [14] reported the seven-layered Aurivillius phases of $Bi_8Fe_{4-x}Co_xTi_3O_{24}$ ($x = 0$–0.4): the highest remanent magnetization of 0.69 emu/g was observed with $x = 0.4$. The Aurivillius phases $Bi_9Fe_{4.7}Me_{0.3}Ti_3O_{27}$ (Me = Fe, Co, Ni, Mn) obtained by Wang et al. [15] demonstrate the highest remanent magnetization in Ni-containing composition.

While the incorporation of cobalt and nickel into Aurivillius phases improves the magnetic parameters, their ferroelectric properties tend to deteriorate, according to most authors [10–13]. This results in a decrease of the remanent polarization; the exceptions were reported by Lei et al. [14] and Wang et al. [15]. Although the doping with cobalt and nickel tends to have a negative impact on the ferroelectric characteristics, these materials belong to a class of the high-temperature multiferroics with ferroelectric and ferromagnetic phase transition temperatures of ~ 780 and ~ 480 °C, respectively. Therefore, they may have potential applications, which include magnetic field sensors, multiple-state memory elements and microwave-integrated circuits. However, the functional properties of single-phase multiferroics need to be improved before practical use. The viability prospects of single-phase multiferroics and the problems encountered have been summarized in the reviews by Scott [16] and Cheng et al. [17].

According to the studies discussed above [10–15], while the substitution of the triple-charged Fe^{3+} cations with the double-charged Co^{2+} and/or Ni^{2+} cations ($Bi_6Fe_{2-x}Co_{x/2}Ni_{x/2}Ti_3O_{18}$ ($0 \le x \le 1$), [10]; $Bi_6Fe_{2-x}Co_xTi_3O_{18}$

(x=0–1), [11]; $Bi_4NdTi_3Fe_{1-x}Co_xO_{15}$ (x=0.1, 0.3, 0.5 и 0.7), [12]; $Bi_5Ti_3Fe_{0.5}Ni_{0.5}O_{15}$, [13]; $Bi_8Fe_{4-x}Co_xTi_3O_{24}$ (x=0–0.4), [14]; $Bi_9Fe_{4.7}Me_{0.3}Ti_3O_{27}$ (Me=Fe, Co, Ni, Mn), [15]) clearly causes the deviation from stoichiometry, it does not lead to the formation of the secondary phases in the samples even at high doping levels. At the same time, there is an evidence that if the Fe^{3+} ion is substituted by double-charged cations, in particular, Co^{2+}, the structure of Aurivillius phases evolves. For example, Zhang et al. [18] have reported that four-layered solid solutions of $Bi_4NdTi_3Fe_{1-x}Co_xO_{15}$ evolve into three-layered $Bi_3NdTi_2CoO_{12-\delta}$ products with the increasing cobalt content. Moreover, careful examination of the low-angle region of the XRD patterns ($2\Theta<20°$) reported by Wang et al. [10] casts doubt on the successful synthesis of solid solutions $Bi_6Fe_{2-x}Co_{x/2}Ni_{x/2}Ti_3O_{18}$ in the entire range of x=0–1. Unfortunately, in a majority of the studies reported, the low-angle region is of poor visibility or not considered.

It is, therefore, clear from the literature that the B-site doping with magnetoactive cations is a viable strategy to improve characteristics of Aurivillius-type layered perovskites $Bi_{m+1}Fe_{m-3}Ti_3O_{3m+3}$ and related compounds. However, within the literature for this family of multiferroics, the electric and magnetic properties reported are mostly studied separately, and little data are available on magnetoelectric properties. The question of whether or not the coupling between the electric and magnetic ordering is strong remains, therefore, unanswered, and extensive further studies are required. Additionally, while understanding the phase-formation processes during the synthesis of Aurivillius phases is of crucial importance for preparation of single-phase materials, this issue has not been given due attention.

In this paper, we have studied the phase-formation processes during the synthesis of Aurivillius structures doped with the magnetoactive nickel cations:

1. $Bi_5Ti_2(TiFe)_{1-x}(NiNb)_xO_{15}$, x=0–1;
2. $Bi_4Ti_{3-2.5x}(Nb_{1/2}Fe_{1/2})_x(Nb_{2/3}Ni_{1/3})_{1.5x}O_{12}$, x=0–0.4;
3. $Bi_3Ti_{1-2.5x}Nb_{1+1.5x}(Fe_{1/2}Ni_{1/2})_xO_9$, x=0–0.3;
4. $Bi_{m+1}Fe_{m-3}Ti_{(3-x)}(Ni_{1/3}Nb_{2/3})_xO_{3m+3}$, m = 4–12, x=0–0.07.

We have investigated the piezoelectric, magnetic, and magnetodielectric (MDE) properties of solid solutions. To avoid the deviation from stoichiometry for all the samples, the mixed cations were selected such that their resulting charge was equal to the charge of the substituted cation.

2 Experimental

Bi_2O_3, Nb_2O_5, NiO, Fe_2O_3, TiO_2 were used as the starting materials for the synthesis of solid solutions in the series (1)–(4). The materials were synthesized using a solid-state method at 800 °C for 8 h with intermediate grinding and sintered at 900 °C for 2 h.

The X-ray powder diffraction analysis of phase composition and calculation of the unit cell parameters was performed using an ARL X'TRA diffractometer with CuK_α-radiation. For calculation of the unit cell parameters, the internal standard was used: the powders of synthesized materials were mixed with macrocrystalline Al_2O_3; the lattice constants were refined using the CELREF software [19].

To determine the Curie (Neel) temperature, the single-phase ceramics were analysed by differential scanning calorimetry (DSC) using a thermal analyzer NETZSCH STA 449 C. The samples were placed in alumina crucibles and heated in air with a rate of 5°/min in the temperature range from 100 to 900 °C.

The magnetic parameters of the samples were measured using a LakeShore VSM 7404 vibration magnetometer at room temperature.

Piezoelectric coefficient d_{33} was measured using a quasi-static d_{33}-meter. The pulse polarization was applied to the samples using a field of 2–4 kV/cm for 3 min in a chloroform medium before measurement.

Temperature and frequency dependence of dielectric constant and dielectric loss tangent in a DC magnetic field of ~ 1 T and in a zero field were investigated using a E7-20 LCR meter in the temperature range of 20–900 °C and frequency range from 20 Hz to 20 MHz.

3 Results and discussion

Figure 2 shows the XRD patterns of the $Bi_5Ti_2(TiFe)_{1-x}(NiNb)_xO_{15}$ samples with x=0.02–1 compared with the standard patterns of the layered Aurivillius phases $Bi_{m+1}Fe_{m-3}Ti_3O_{3m+3}$ (m=3 and 4) from ICDD. It could be observed that the mixed cation $(Ni_{1/2}Nb_{1/2})^{3.5+}$ does not dissolve in the B-sublattice of the four-layered $Bi_5Ti_3FeO_{15}$ with $x\geq0.2$. With x=0.2–0.4, there are the peaks of the secondary phase of the $Bi_4Ti_3O_{12}$-derived three-layered perovskite. There is an unidentified phase in the XRD patterns, which is represented only by an intense single peak near $2\Theta\approx28°$. With x=0.6, in addition to the three-layered phase, there are the peaks of the secondary phase corresponding to the two-layered perovskite-type compound Bi_3TiNbO_9. The amount of the two-layered phase increases with x=0.8, and with x=1, the two-layered phase dominates. Thus, the doping of four-layered perovskite $Bi_5Ti_3FeO_{15}$ with a significant concentration of the mixed cation $(Ni_{1/2}Nb_{1/2})^{3.5+}$ leads to its destabilization and decomposition into two- and three-layered products. However, with $x\leq0.1$, solid solutions of the $Bi_5Ti_2(TiFe)_{1-x}(NiNb)_xO_{15}$ system are formed according to the XRD patterns (Fig. 2). The samples contain no impurity

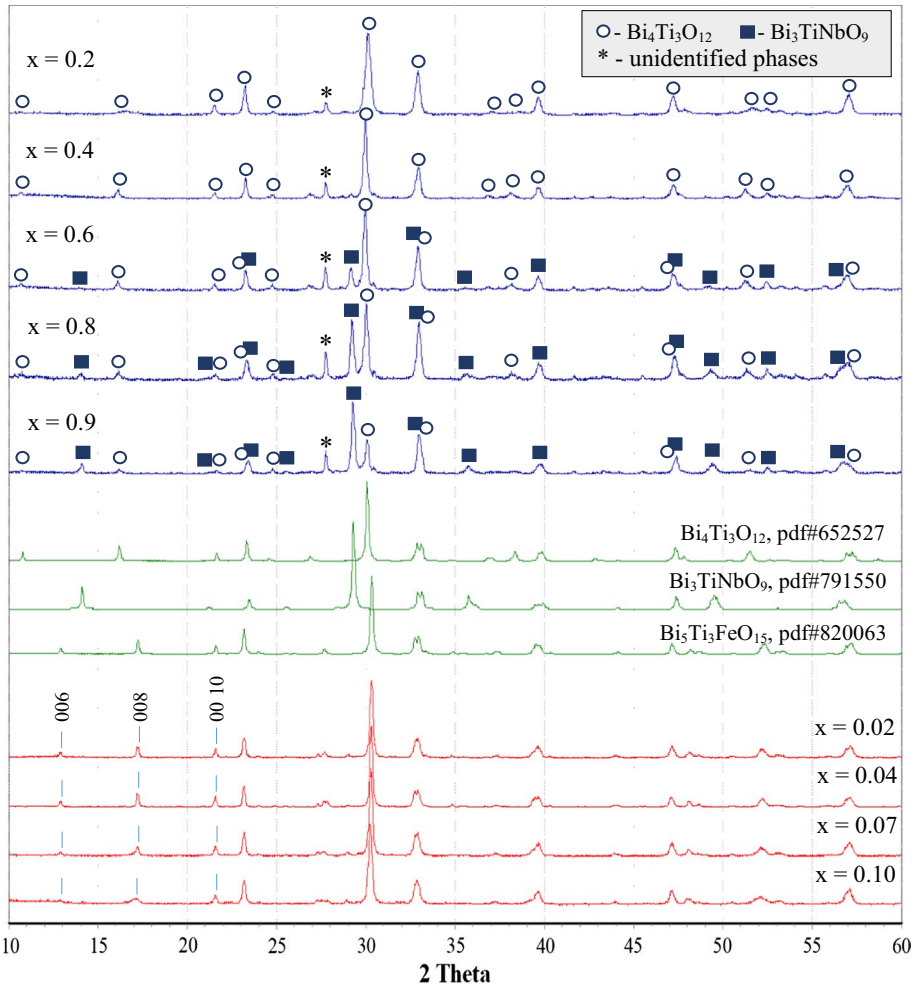

Fig. 2 XRD patterns of the $Bi_5Ti_2(TiFe)_{1-x}(NiNb)_xO_{15}$ samples and the standard patterns of $Bi_4Ti_3O_{12}$, Bi_3TiNbO_9, $Bi_5Ti_3FeO_{15}$ from ICDD. For single-phase products with $x \leq 0.01$, the short lines indicate a shift of the peaks (*001*) to lower 2θ with increasing x

phases. Moreover, the clear shift of the peaks with the (00 *l*) Miller indices (peaks in the range of $2\Theta \approx 8$–$22°$) to lower angles with increasing x is the evidence of the formation of solid solutions, which indicates the incorporation of the larger cations $(Ni_{1/2}Nb_{1/2})^{3.5+}$ into the B-sublattice of layered structure. Indeed, according to Shannon [20], the ionic radii of six-coordinated cations are: $r(Ti^{4+}) = 0.745$ Å, $r(Ni^{2+}) = 0.83$ Å, $r(Nb^{5+}) = 0.78$ Å, $r(Fe^{3+}) = 0.785$ Å (for high-spin state); i.e. $r((Ni_{1/2}Nb_{1/2})^{3.5+}) = 0.805$ Å, which is larger than $r((Fe_{1/2}Ti_{1/2})^{3.5+}) = 0.765$ Å. Figure 3a, b shows the concentration dependence of the parameters and volumes of the orthorhombic unit cells for single-phase $Bi_5Ti_2(TiFe)_{1-x}(NiNb)_xO_{15}$ in the range of $x = 0$–0.1. We have observed an increase in the parameters *a, b* and *c*, which increases the volume of the unit cell.

The results of the experiments with the four-layered $Bi_5Ti_2(TiFe)_{1-x}(NiNb)_xO_{15}$ suggest that the layered phases with a smaller number of layers in perovskite blocks are more tolerant to doping with mixed cations. We have doped the Bi_3TiNbO_9 and $Bi_4Ti_3O_{12}$ compounds with magnetoactive cations in accordance with the formulae $Bi_3Ti_{1-2.5x}Nb_{1+1.5x}(Fe_{1/2}Ni_{1/2})_xO_9$ and $Bi_4Ti_{3-2.5x}(Nb_{1/2}Fe_{1/2})_x(Nb_{2/3}Ni_{1/3})_{1.5x}O_{12}$ in the range $x = 0$–0.4. In both cases, the Ti^{4+} cation was substituted by mixed cation $(Nb_{3/5}Fe_{1/5}Ni_{1/5})^{4+}$.

Figure 4a shows the XRD patterns of $Bi_3Ti_{1-2.5x}Nb_{1+1.5x}(Fe_{1/2}Ni_{1/2})_xO_9$ system with $x = 0$–0.4. According to the experimental data, solid solutions are formed in the range of $x = 0$–0.3. Thus, it was confirmed that the two-layered perovskite Bi_3TiNbO_9 is more tolerant to doping with mixed cation than $Bi_5Ti_3FeO_{15}$. With $x = 0.4$, the peaks of the secondary phase, apparently with the pyrochlore structure, appear. For the single-phase products of the $Bi_3Ti_{1-2.5x}Nb_{1+1.5x}(Fe_{1/2}Ni_{1/2})_xO_9$ system, the lattice constants are refined, and the volumes of unit cells are calculated (Fig. 5a, b). All the lattice constants and, consequently, the volumes of the unit cells increase, which is in good agreement with the ionic radii: $r((Nb_{3/5}Fe_{1/5}Ni_{1/5})^{4+}) = 0.791$ Å is larger than that of Ti^{4+} (0.745 Å).

Figure 4b shows the XRD patterns of the samples of the $Bi_4Ti_{3-2.5x}(Nb_{1/2}Fe_{1/2})_x(Nb_{2/3}Ni_{1/3})_{1.5x}O_{12}$ system with $x = 0$–0.4 and layered Aurivillius phase of $Bi_{m+1}Fe_{m-3}Ti_3O_{3m+3}$ with $m = 3$ from ICDD. Obviously, the solid solutions are formed in this system in a narrower range

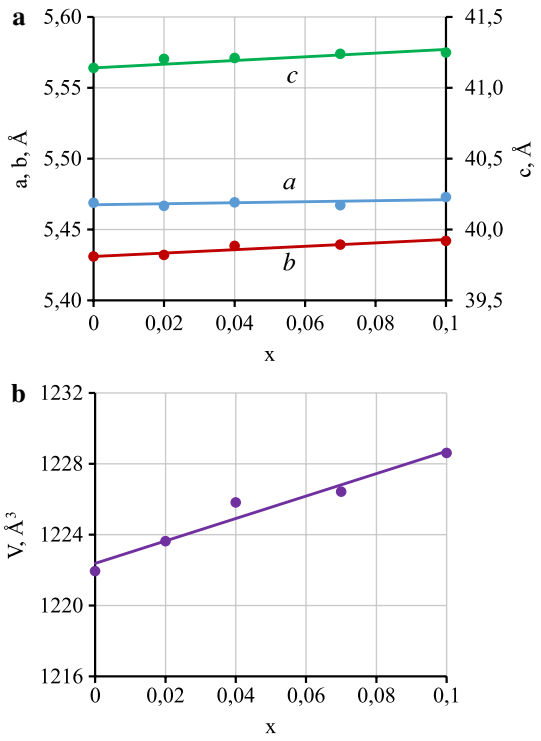

Fig. 3 **a** Parameters and **b** volumes of $Bi_5Ti_2(TiFe)_{1-x}(NiNb)_xO_{15}$ unit cells

of $x = 0$–0.2, and the peaks of impurity phases appear with $x \geq 0.3$. An increase in lattice constants and volumes of unit cells was observed due to the incorporation of larger cations $(Nb_{3/5}Fe_{1/5}Ni_{1/5})^{4+}$ into the B-sublattice (Fig. 6a, b).

For the Ni-containing Aurivillius phases with a respective number of layers m in perovskite blocks, the effect of heterovalent doping on the stability was investigated. For this purpose, we have studied several $Bi_{m+1}Fe_{m-3}Ti_{(3-x)}(Ni_{1/3}Nb_{2/3})_xO_{3m+3}$ solid solutions similar to the layered perovskites described above. The single-phase samples could be obtained at $x = 0$–0.07 and $m \leq 6$–7 (Fig. 7). The samples with $m > 7$ contain some impurity phases such as $Bi_2Fe_4O_9$ and Bi_2O_3-derived cubic phase. In the $Bi_{m+1}Fe_{m-3}Ti_3O_{3m+3}$ system, according to the previously reported data [5], the single-phase samples could be synthesized up to $m = 8$ in the absence of the $[Ni_{1/3}Nb_{2/3}]^{4+}$ dopant. Thus, the introduction of the dopant decreases the stability of Aurivillius phases only slightly. Figure 8 shows the dependence of the parameters and volumes of the orthorhombic unit cells of $Bi_{m+1}Fe_{m-3}Ti_{(3-x)}(Ni_{1/3}Nb_{2/3})_xO_{3m+3}$ with $x = 0.05$ on m, similar trends were observed for the samples with $x = 0.03$ and 0.07. According to these graphs, the increasing m value results in an almost linear increase in parameters *a, b, c* of the unit cells. Additionally, an increase in the concentration of $Ni_{1/3}Nb_{2/3}$ (x) dopant leads to an increase in all parameters of the $Bi_{m+1}Fe_{m-3}Ti_{(3-x)}(Ni_{1/3}Nb_{2/3})_xO_{3m+3}$ unit cells in the whole range of m. This dependence is expected since the ionic radius of the dopant $r(Ni_{1/3}Nb_{2/3})^{4+}) = 0.797$ Å is larger than the radius of the substituted ion $r(Ti^{4+}) = 0.745$ Å. The observed dependences of the lattice constants on the number of perovskite layers can be described by linear equations with high Pearson coefficients: with $x = 0.05$ $a = 0.012\ m + 5.387$ ($R^2 = 0.983$), $b = 0.016\ m + 5.395$ ($R^2 = 0.991$), $c = 8.274\ m + 8.448$ ($R^2 = 0.999$). The linear increase in c indicates that the perovskite fragment embedded in the structure of the layered compound undergoes minimal changes along the c axis with increasing m. The coefficients in the function $c(m)$ allow estimating the thickness of the perovskite layer in the studied homological series $Bi_{m+1}Fe_{m-3}Ti_{(3-x)}(Ni_{1/3}Nb_{2/3})_xO_{3m+3}$: with $x = 0.05$, the thickness is equal to 4.137 Å. This value is slightly higher than expected from the ionic radii of the respective cations. If $r(Bi^{3+}) = 1.59$ Å and $r(O^{2-}) = 1.26$ Å, the thickness of the perovskite layer is 3.96 Å. At the same time, with small m values, a base area of the unit cell ($S^2 = ab = 0.000192\ m^{2+} 0.150932\ m + 29.062865$) is noticeably smaller than that of pure bismuth ferrite (with $m = 3$, the base area is equal to 29.517 $Å^2$, while for $BiFeO_3$ it is $(3{,}96 \cdot \sqrt{2})^2 = 31.363\ A^2$). Thus, the perovskite-type unit cell of Aurivillius phases studied is compressed along the a and b directions and stretched along the c axis in the whole range of m.

One of the major problems with all single-phase products obtained in this study is the high electrical conductivity that inhibits the development of the hysteresis loops and seriously affects the polarization of the ceramics. Nevertheless, the ceramics can be polarized: the single-phase samples of all the studied systems, except the two-layered $Bi_3Ti_{1-2.5x}Nb_{1+1.5x}(Fe_{1/2}Ni_{1/2})_xO_9$ solid solutions, demonstrate the piezoelectric properties at room temperature; the average values of d_{33} and g_{33} are 1.5–2 pC/N and 0.5–1 mV m/N and up to 7 pC/N and 3.5 mV m/N in the best samples. For the samples of $Bi_3Ti_{1-2.5x}Nb_{1+1.5x}(Fe_{1/2}Ni_{1/2})_xO_9$ and $Bi_4Ti_{3-2.5x}(Nb_{1/2}Fe_{1/2})_x(Nb_{2/3}Ni_{1/3})_{1.5x}O_{12}$, magnetic hysteresis loops were not observed. For other compounds, there is a general trend of the increasing saturation magnetization and remanent magnetization with the increasing dopant concentration, while the coercivity remains almost unchanged. This trend is demonstrated in Fig. 9 using the $Bi_5Ti_2(TiFe)_{1-x}(NiNb)_xO_{15}$ samples as an example.

The ferroelectric (antiferroelectrics) and ferromagnetic (antiferromagnetic) compounds are known to exhibit their properties in a specific temperature range and shift to paraelectric or paramagnetic state, respectively, at the Curie (Neel) point, which can be accompanied by thermal effects. The DSC method was used for thermal studies in the single-phase ceramic samples of the series (1) and (4) with both the piezoelectric and magnetic properties. Figure 10 shows the DSC curves of the $Bi_5Ti_2(TiFe)_{1-x}(NiNb)_xO_{15}$

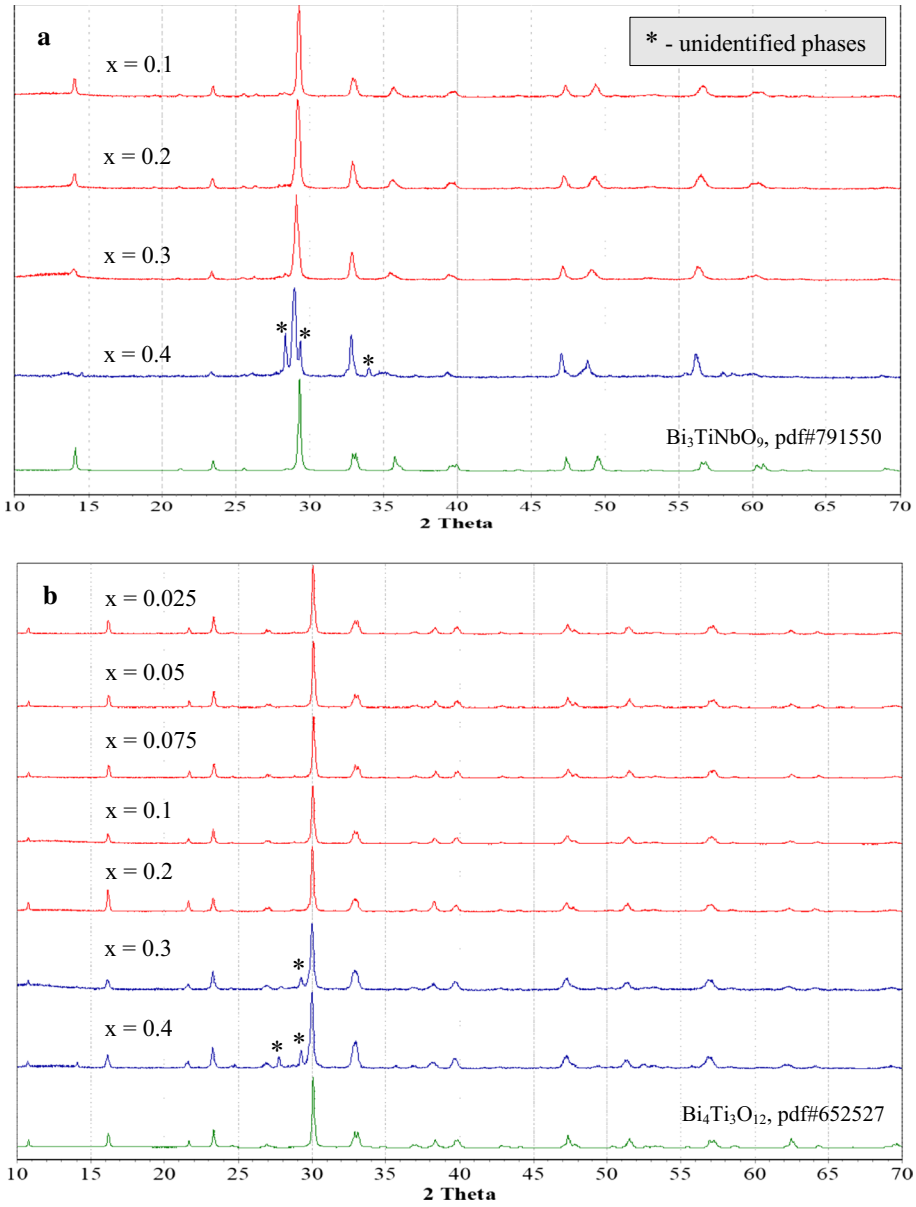

Fig. 4 **a** XRD patterns of $Bi_3Ti_{1-2.5x}Nb_{1+1.5x}(Fe_{1/2}Ni_{1/2})_xO_9$, **b** $Bi_4Ti_{3-2.5x}(Nb_{1/2}Fe_{1/2})_x(Nb_{2/3}Ni_{1/3})_{1.5x}O_{12}$ and the standard patterns of Bi_3TiNbO_9 and $Bi_4Ti_3O_{12}$ from ICDD

samples. The shape of the DSC curves is typical for all the samples (1) and (4). The shape of the curves corresponds to several thermal events: a series of low-temperature effects in the range of ~ 300–400 °C and two high-temperature anomalies at 750 and 840 °C. According to the previously reported data, we could propose that the first of the two high-temperature thermal effects refers to the ferroelectric Curie point, which in good agreement with the undoped compositions of the $Bi_4Ti_3O_{12}$–$BiFeO_3$ [5] system. The temperature of the second high-temperature effect is close to the ferroelectric Curie point of $BiFeO_3$ (~ 850 °C, [6]) and, probably, has a ferroelectric nature. Finally, in the range of ~ 300–400 °C, the DSC curves of the samples show significant anomalies that could be attributed to the magnetic properties, which is in good agreement with the antiferromagnetic point of $BiFeO_3$ (~ 370 °C [6]). Similar DSC curves were obtained for the single-phase products of the $Bi_{m+1}Fe_{m-3}Ti_{(3-x)}(Ni_{1/3}Nb_{2/3})_xO_{3m+3}$ series.

The temperature and frequency dependencies of the dielectric properties of the ceramic samples were studied to clarify the nature of low-temperature thermal effects. Figure 11 shows the temperature dependence of the dielectric constant $\varepsilon/\varepsilon_0$ and dielectric loss tangent $\tan\delta$ of the $Bi_{m+1}Fe_{m-3}Ti_{(3-\delta)}(Ni_{1/3}Nb_{2/3})_\delta O_{3m+3}$ sample with $m = 5$,

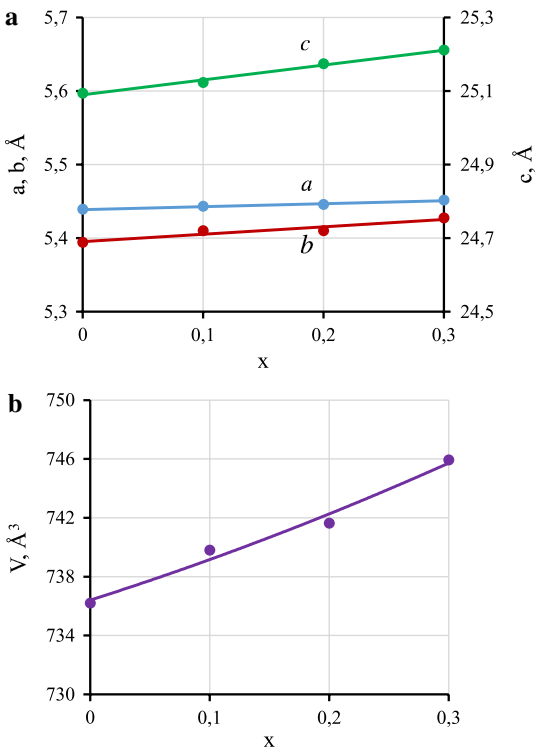

Fig. 5 **a** Parameters and **b** volumes of the $Bi_3Ti_{1-2.5x}Nb_{1+1.5x}(Fe_{1/2}Ni_{1/2})_xO_9$ unit cells

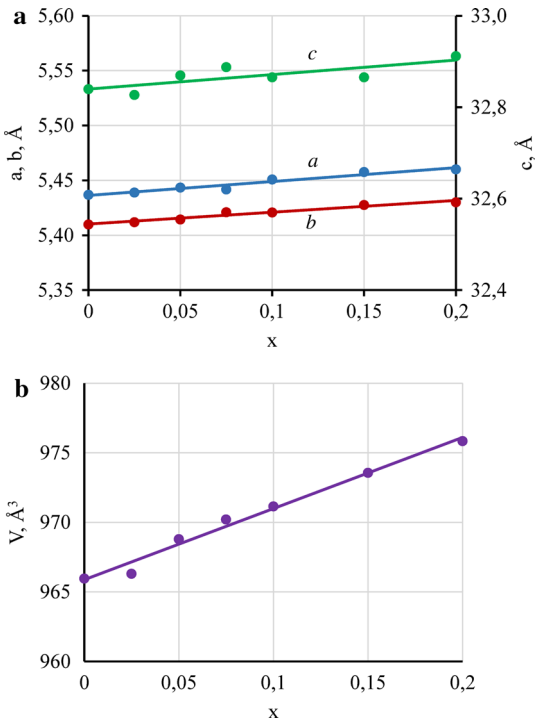

Fig. 6 **a** Parameters and **b** volumes of the $Bi_4Ti_{3-2.5x}(Nb_{1/2}Fe_{1/2})_x(Nb_{2/3}Ni_{1/3})_{1.5x}O_{12}$ unit cells

$x = 0.05$ (recorded on heating). An increase in temperature above 400 °C results in an increase in the electrical conductivity, and the further measurements become impossible. As shown in Fig. 11, the dependencies $\varepsilon/\varepsilon_0(T)$ and $\tan\delta(T)$ have no anomalies with a zero magnetic field, while in a DC magnetic field, $\varepsilon/\varepsilon_0$(T) and $\tan\delta(T)$ take the maxima at the temperature of ~ 340 °C. In addition, the values $\varepsilon/\varepsilon_0$ and $\tan\delta$ increase in a DC magnetic field: for example, at a frequency of 1 kHz at 340 °C, $\varepsilon/\varepsilon_0 = 250$ and 365, $\tan\delta = 0.59$ and 0.91 in a zero and 1 T magnetic field, respectively. Probably, at 340 °C (which is close to the Curie point of bismuth ferrite) the $Bi_{m+1}Fe_{m-3}Ti_{(3-x)}(Ni_{1/3}Nb_{2/3})_xO_{3m+3}$ material with $m = 5$, $x = 0.05$ undergoes a phase transition that has a magnetic nature, which induces the anomalies in dielectric properties. Thus, the resulting materials show the magnetodielectric (MDE) effect with a maximum value of ~ 50%. As is known, the materials with high MDE are promising for practical applications in various devices such as capacitive, magnetic field sensors, tunable microwave filters, etc. La_2NiMnO_6 [21] is one of the most effective magnetodielectric materials, which exhibits the room temperature MDE of ~ 16% in a field of ~ 2 T. However, the MDE effect in Aurivillius phases is relatively small at room temperatures and does not exceed ~ 1%. The observed MDE, however, experimentally confirms the existence of a coupling between the electric and magnetic ordering in Aurivillius phases containing magnetoactive cations, which makes these materials interesting from both the fundamental and practical points of view.

4 Conclusions

The phase-formation processes during the solid-state synthesis and a range of single-phase existence were studied in Aurivillius structures (1) $Bi_5Ti_2(TiFe)_{1-x}(NiNb)_xO_{15}$, (2) $Bi_4Ti_{3-2.5x}(Nb_{1/2}Fe_{1/2})_x(Nb_{2/3}Ni_{1/3})_{1.5x}O_{12}$, (3) $Bi_3Ti_{1-2.5x}Nb_{1+1.5x}(Fe_{1/2}Ni_{1/2})_xO_9$, (4) $Bi_{m+1}Fe_{m-3}Ti_{(3-x)}(Ni_{1/3}Nb_{2/3})_xO_{3m+3}$. The range of existence of solid solutions was found to be limited to the values of $x = 0$–0.10 (1), 0–0.3 (2), and 0–0.2 (3). The unit cell volumes increase with increasing x, which is expected due to the ionic radii of the dopant cations that are larger than those of the substituted cations. Although the solid solutions exist in the whole concentration range studied ($x = 0$–0.07) in the series (4), the stability is limited to the value of $m = 6$–7. The samples with $m > 7$ contain some impurity phases such as $Bi_2Fe_4O_9$ and Bi_2O_3-derived cubic phase. The coexistence of piezoelectric and magnetic properties was observed in the samples of solid solutions (1) and (4): the values of the piezoelectric coefficient d_{33} and piezoelectric voltage coefficient g_{33} reach 7 pC/N and 3.5 mV m/N, respectively; the saturation magnetization M_s and remanent magnetization M_r increase with increasing x, while

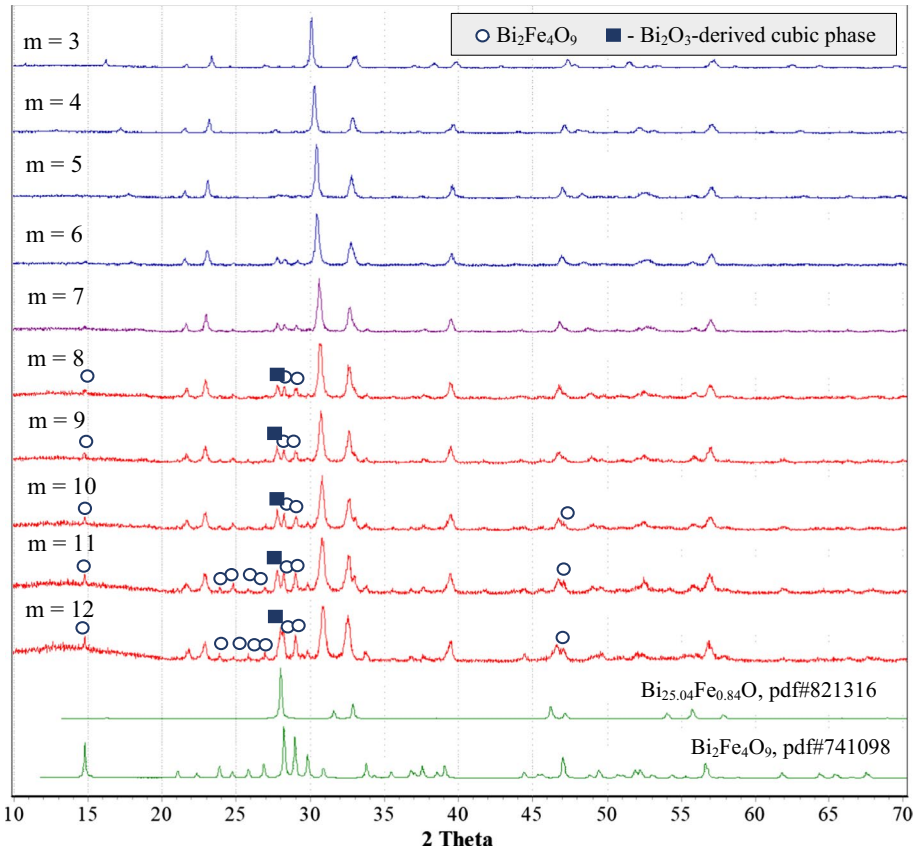

Fig. 7 **a** XRD patterns of $Bi_{m+1}Fe_{m-3}Ti_{(3-x)}(Ni_{1/3}Nb_{2/3})_xO_{3m+3}$ with $x=0.05$ and the standard patterns of $Bi_2Fe_4O_9$ and $Bi_{25.04}Fe_{0.84}O_{40}$ from ICDD

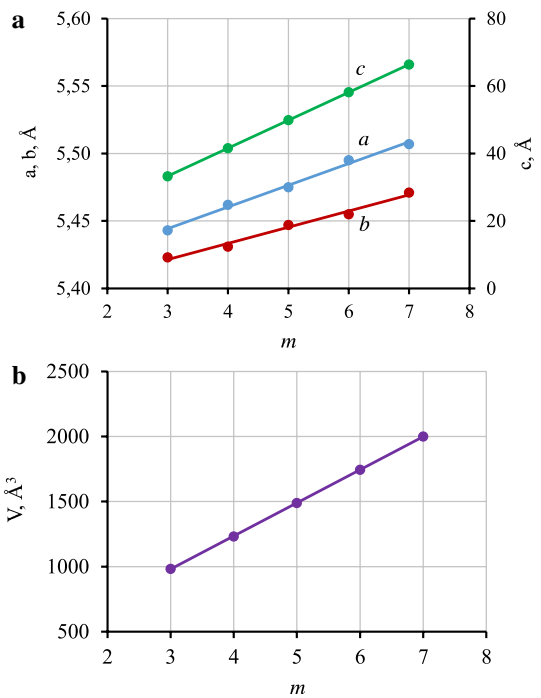

Fig. 8 **a** Parameters and **b** volumes of the $Bi_{m+1}Fe_{m-3}Ti_{(3-x)}(Ni_{1/3}Nb_{2/3})_xO_{3m+3}$ ($x=0.05$) unit cells

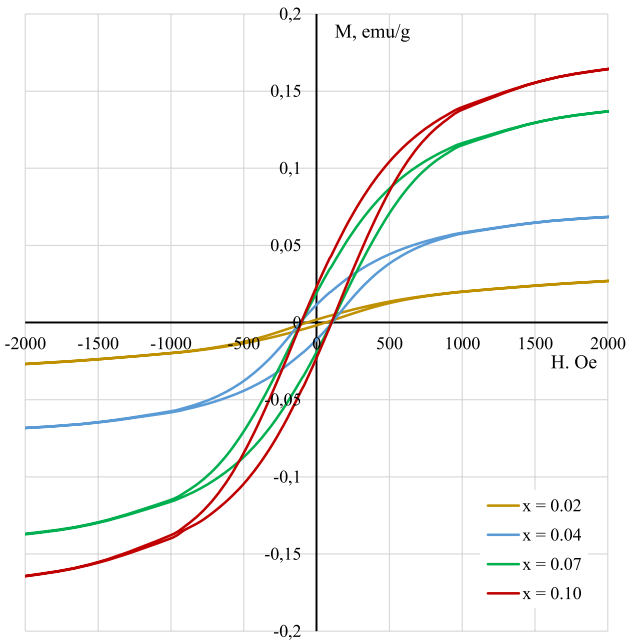

Fig. 9 M–H loops for solid solutions of $Bi_5Ti_2(TiFe)_{1-x}(NiNb)_xO_{15}$

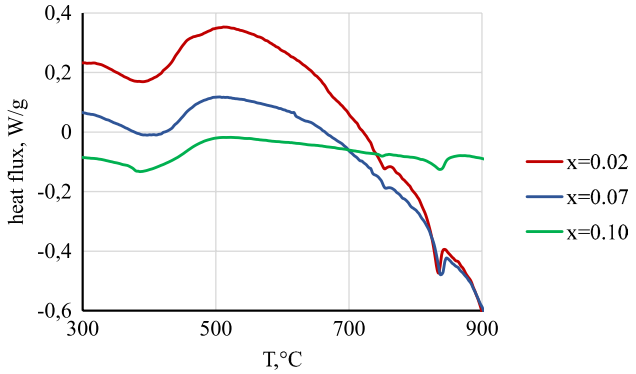

Fig. 10 DSC curves for the $Bi_5Ti_2(TiFe)_{1-x}(NiNb)_xO_{15}$ samples

the coercivity remains almost unchanged. Thermal studies indicate phase transitions in $Bi_5Ti_2(TiFe)_{1-x}(NiNb)_xO_{15}$, and $Bi_{m+1}Fe_{m-3}Ti_{(3-x)}(Ni_{1/3}Nb_{2/3})_xO_{3m+3}$ at ~ 300–400, 750 and 840 °C. It is particularly important that the samples demonstrate a magnetodielectric effect of up to ~ 50% when applying a DC magnetic field of 1 T in the temperature range of ~ 340–350 °C that is supposed to be a ferromagnetic Curie point. The observed MDE indicates a coupling between the electric and magnetic ordering, which makes the studied Aurivillius phases interesting from both the fundamental and practical points of view.

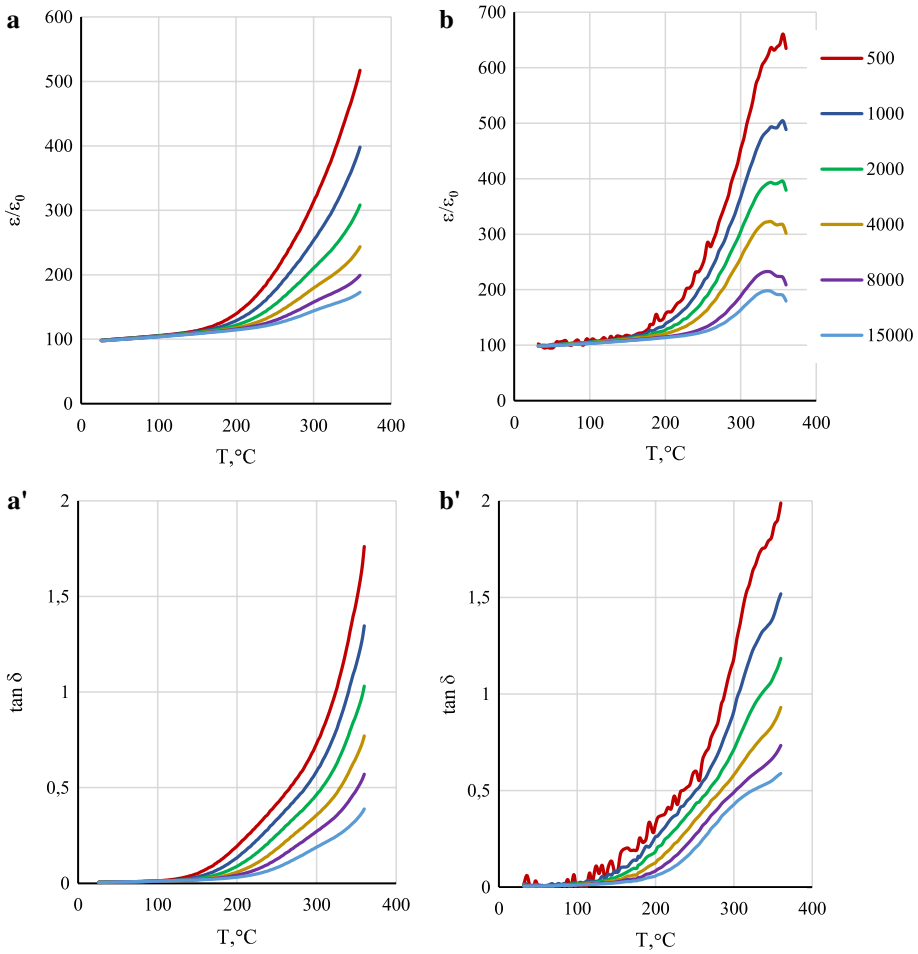

Fig. 11 Temperature dependence of dielectric constant and dielectric loss tangent (recorded during heating) at different frequencies (Hz) for the $Bi_{m+1}Fe_{m-3}Ti_{(3-x)}(Ni_{1/3}Nb_{2/3})_xO_{3m+3}$ ($m=5$, $x=0.05$) sample. a and a' correspond to a zero magnetic field; b and b' correspond to a DC magnetic field of ~ 1 T

Acknowledgements The authors express their appreciation to the Deanship of Scientific Research at King Khalid University for funding this work through research groups programme under grant number R.G.P.1/12/39.

References

1. B. Aurivillius, Ark. Kemi. **54**, 463 (1949)
2. B. Aurivillius, Ark. Kemi. **58**, 499 (1949)
3. B. Aurivillius, Ark. Kemi. **37**, 512 (1950)
4. G.A. Smolensky, V.A. Isupov, A.I. Agranovskaya, Soviet. Phys. Solid State **1**, 169 (1959)
5. N.A. Lomanova, M.I. Morozov, V.L. Ugolkov, V.V. Gusarov, Inorg. Mater. **42**, 189 (2006)
6. Y. Venevtsev, E.D. Politova, S.A. Ivanov, *Ferro- and Antiferroelectrics of the Barium Titanate Family* (Khimiya, Moscow, 1985), pp. 193–197
7. A. Srinivas, D.-W. Kim, K.S. Hong, S.V. Suryanarayana, Mater. Res. Bull. **39**, 55 (2004). https://doi.org/10.1016/j.materresbull.2003.09.028
8. A. Srinivas, F. Boey, T. Sritharan, D.W. Kim, K.S. Hong, S.V. Suryanarayana, Ceram. Int. **30**, 1431 (2004). https://doi.org/10.1016/j.ceramint.2003.12.074
9. N. Prasad, G. Kumar, J. Magn. Magn. Mater. **213**, 349 (2000). https://doi.org/10.1016/S0304-8853(99)00849-5
10. T. Wang, H. Deng, X. Meng, H. Cao, W. Zhou, P. Shen, Y. Zhang, P. Yang, J. Chu, Ceram. Int. **43**, 8792 (2017). https://doi.org/10.1016/J.CERAMINT.2017.04.010
11. Z. Liu, J. Yang, X.W. Tang, L.H. Yin, X.B. Zhu, J.M. Dai, Y.P. Sun, Appl. Phys. Lett. **101**, 122402 (2012). https://doi.org/10.1016/J.PHYSLETA.2018.12.031
12. Y. Shu, Q. Ma, Z. Ding, L. Cao, X. Chen, F. Yang, X. Zeng, Phys. Lett. A **383**, 911 (2019). https://doi.org/10.1016/j.ceramint.2013.10.063
13. X. Chen, J. Xiao, Y. Xue, X. Zeng, F. Yang, P. Su, Ceram. Int. **40**, 2635 (2014). https://doi.org/10.3390/cryst7030076
14. Z. Lei, T. Chen, W. Li, M. Liu, W. Ge, Y. Lu, Crystals. **7**, 76 (2017). https://doi.org/10.1007/s11434-014-0625-7
15. G. Wang, S. Sun, Y. Huang, J. Wang, R. Peng, Z. Fu, Y. Lu, Chin. Sci. Bull. **59**, 5199 (2014). https://doi.org/10.1039/c2jm16137k
16. J.F. Scott, J. Mater. Chem. **22**, 4567 (2012). https://doi.org/10.1039/c2jm16137k
17. Y. Cheng, B. Peng, Z. Hu, Z. Zhou, M. Liu, Phys. Lett. Sect. A. Gen At Solid State Phys. **382**, 3018 (2018). https://doi.org/10.1016/j.physleta.2018.07.014
18. D.L. Zhang, W.C. Huang, Z.W. Chen, W.B. Zhao, L. Feng, M. Li, Y.W. Yin, S.N. Dong, X.G. Li, Sci. Rep. **7**, 43540 (2017). https://doi.org/10.1016/j.physleta.2018.07.014
19. J. Laugier, B. Bochu, CELREF3 unit cell refinement software. http://www.ccp14.ac.uk/tutorial/lmgp/celref.htm. Accessed 4 Aug 2019
20. R.D. Shannon, Database of Ionic Radii. http://abulafia.mt.ic.ac.uk/shannon/ptable.php. Accessed 10 Oct 2019
21. D. Choudhury, P. Mandal, R. Mathieu, A. Hazarika, S. Rajan, A. Sundaresan, U.V. Waghmare, R. Knut, O. Karis, P. Nordblad, D.D. Sarma, Phys. Rev. Lett. **108**, 127201 (2012). https://doi.org/10.1103/PhysRevLett.108.127201

Publisher's Note Springer Nature remains neutral with regard to jurisdictional claims in published maps and institutional affiliations.